



Published in final edited form as:

Nat Nanotechnol. 2014 March ; 9(3): 204–210. doi:10.1038/nnano.2014.17.

## Prevention of Vascular Inflammation by Nanoparticle Targeting of Adherent Neutrophils

Zhenjia Wang<sup>1,2,+</sup>, Jing Li<sup>1</sup>, Jaehyung Cho<sup>1,2,3</sup>, and Asrar B. Malik<sup>1,2,\*</sup>

<sup>1</sup>Department of Pharmacology, University of Illinois Chicago College of Medicine, Chicago, IL 60612

<sup>2</sup>Center for Lung and Vascular Biology, University of Illinois Chicago College of Medicine, Chicago, IL 60612

<sup>3</sup>Department of Anesthesiology, University of Illinois Chicago College of Medicine, Chicago, IL 60612

Inflammatory diseases such as acute lung injury and ischemic tissue injury are caused by the adhesion of a type of white blood cell known as polymorphonuclear neutrophils to the lining of the circulatory system or vascular endothelium, and unchecked neutrophil transmigration<sup>1,2</sup>. Nanoparticle-mediated targeting of activated neutrophils on vascular endothelial cells at the site of injury may be a useful means of directly inactivating neutrophil transmigration, and hence mitigating vascular inflammation<sup>3</sup>. Here we report a method employing drug-loaded albumin nanoparticles that efficiently deliver drugs into neutrophils adherent to the surface of the inflamed endothelium. Using intravital microscopy of tumor necrosis factor- $\alpha$ -challenged mouse cremaster post-capillary venules, we demonstrated that fluorescently-tagged albumin nanoparticles were largely internalized by neutrophils adherent to the activated endothelium via cell surface Fc $\gamma$  receptors. Administration of albumin nanoparticles loaded with the spleen tyrosine kinase inhibitor, piceatannol, which blocks 'outside-in'  $\beta$ 2 integrin signaling in leukocytes, detached the adherent neutrophils and elicited their release into the circulation. Thus, internalization of drug-loaded albumin nanoparticles into neutrophils inactivates the pro-inflammatory function of activated neutrophils, thereby offering a promising approach for treating inflammatory diseases resulting from inappropriate neutrophil sequestration and activation.

Neutrophil adhesion to activated endothelial cells and subsequent trans- endothelial migration are essential events of the innate immune response that eliminate invading pathogens to promote bacterial clearance<sup>4-6</sup>. While neutrophil recruitment into site of injury is the first-line of host defence, excessive neutrophil infiltration and activation at the vessel

Users may view, print, copy, and download text and data-mine the content in such documents, for the purposes of academic research, subject always to the full Conditions of use:[http://www.nature.com/authors/editorial\\_policies/license.html#terms](http://www.nature.com/authors/editorial_policies/license.html#terms)

\*To whom correspondence should be addressed: Asrar B. Malik, abmalik@uic.edu.

<sup>†</sup>Present address: Department of Pharmaceutical Sciences, Washington State University, Spokane, WA

**Author Contributions:** Z.W., J.C., and A.B.M. designed the experiments and analyzed the data; Z.W. and J.L. carried out the experiments; Z.W., J.C., and A.B.M. wrote the manuscript.

Supplementary information accompanying this paper can be found at [www.nature.com/naturenanotechnology](http://www.nature.com/naturenanotechnology).

**Competing Financial Interests:** The authors declare no competing financial interests.

wall is also the primary cause of inflammation and tissue damage. Neutrophils have been implicated in numerous inflammatory diseases such as acute lung injury, sepsis, and ischemia-reperfusion injury<sup>1,2,6,7</sup>. Studies showed that inhibition of  $\beta 2$  integrins by anti- $\beta 2$  integrin antibodies blocked the adhesion of neutrophils to endothelial cells, and prevented inflammation, leading to restored vascular integrity<sup>8</sup>. These studies support the concept that targeting neutrophils is a useful strategy; however, antibodies also reduced the bactericidal function of neutrophils by impairing the ability of circulating cells to adhere and migrate to the site of infection<sup>9</sup>.

Nanoparticles have the capability to carry and deliver therapeutics to target cells, due to the coating of ligands and antibodies to their surface<sup>3,10</sup>. For example, promising results have been obtained using nanoparticles to deliver therapeutics into tumours using cell surface antigens as targeting “addresses”<sup>11,12</sup>. In this report, using real-time intravital microscopy of the inflamed post-capillary venules of live mice, the primary site of neutrophil adhesion and extravasation in the circulation<sup>13,14</sup>, we demonstrate that albumin nanoparticles are internalized by activated neutrophils through endocytosis, which is in part mediated by Fc $\gamma$  receptor (Fc $\gamma$ R) III. The treatment of mice with albumin nanoparticles incorporating piceatannol, an inhibitor for spleen tyrosine kinase (Syk that blocks ‘outside-in’ integrin signaling<sup>15</sup>, markedly reduced neutrophil adhesion and migration across the endothelium. Studies in a mouse model of endotoxin-induced acute lung injury, mediated by the infiltration of neutrophils, also showed that piceatannol-incorporated albumin nanoparticles prevented lung injury.

We prepared stable albumin nanoparticles by desolvation of bovine serum albumin (BSA) using ethanol, followed by albumin cross-linking using glutaraldehyde (Supplementary Fig. S1)<sup>16</sup>. To study the internalization properties of albumin nanoparticles by phagocytes, we incorporated fluorescent dyes into nanoparticles (Supplementary Fig. S1). Studies using transmission electron microscopy (Supplementary Fig. S2) and dynamic light scattering (Supplementary Fig. S3) showed that the size of albumin nanoparticles with and without fluorescent dyes were similar with a mean diameter of  $100 \pm 10$  (SD) nm.

We next employed real-time fluorescence intravital microscopy to study the uptake of albumin nanoparticles by neutrophils<sup>13</sup>. Vascular inflammation was induced by intrascrotal injection of the pro-inflammatory cytokine tumour necrosis factor (TNF- $\alpha$ ) in mice. At 3 hr post-TNF- $\alpha$  challenge, cremaster muscle was exposed, and neutrophils adherent to activated venular endothelial cells were monitored. Intravenous injection of Cy5-loaded albumin nanoparticles resulted in the nanoparticles being largely internalized by the leukocytes adherent to the inflamed venular endothelial cells, and, to some extent, by neutrophils slowly rolling along the vessel wall (Movie 1). However, nanoparticles were not internalized by the TNF- $\alpha$  activated endothelium itself. To confirm that the nanoparticles were primarily internalized by neutrophils, we simultaneously intravenously infused an Alexa Fluor 488-labeled anti-mouse Gr-1 antibody<sup>13</sup> and Cy5-loaded albumin nanoparticles. Anti-mouse Gr-1 antibody and albumin nanoparticles showed marked co-staining (Fig. 1a and Movie 2). In control experiments, non-immune isotype control antibody, IgG did not show any signal (Supplementary Fig. S4). To address whether albumin nanoparticles can also be internalized by unstimulated neutrophils in the circulation, Cy5-loaded albumin nanoparticles were

infused intravenously. Here, using Cy5-loaded albumin nanoparticles, we failed to detect Gr-1 positive neutrophils (Fig. 1b and Movie 3), indicating that only adherent neutrophils were able to internalize the nanoparticles. We also examined nanoparticle internalization by adherent monocytes, another phagocytic cell involved in inflammation<sup>17</sup>. At 3 hr post-intrascrotal injection of TNF- $\alpha$ , Alexa Fluor 488-labeled anti-mouse F4/80 antibody<sup>17</sup> (which marks for monocytes) and Cy5-loaded albumin nanoparticles were infused intravenously, and monitored. Adherent monocytes, unlike neutrophils, did not internalize albumin nanoparticles (Fig. 1c-d and Movie 4).

To investigate essential determinants of nanoparticle internalization, we compared the uptake of three different types of nanoparticles by activated neutrophils. In the first two experiments, BSA nanoparticles were made by ethanol-induced albumin desolvation<sup>16,18</sup> to denature albumin, a process followed by albumin cross-linking to form stable particles (Fig. 2a). Albumin nanoparticles were then either incorporated with fluorescent dye (Cy5-loaded albumin nanoparticles shown in Fig. 1) or their surface was chemically conjugated with Alexa Fluor 647 by a carboxyl-amine reaction that forms covalent bonds between Alexa Fluor 647 and albumin nanoparticles (Alexa Fluor 647-conjugated albumin nanoparticles)<sup>19</sup>. We also fabricated nanoparticles in which yellow-green fluorescence polystyrene nanoparticles with diameter of 100 nm were coated with native BSA (albumin-conjugated polystyrene nanoparticles)<sup>19</sup>. Comparing the uptake of these two types of albumin nanoparticles by Gr-1 positive neutrophils following intravenous infusion at 3 hr after intrascrotal injection of TNF- $\alpha$ , we observed that Alexa Fluor 647-conjugated albumin nanoparticles were internalized by the adherent neutrophils and showed characteristic punctual distribution in the cytosol, whereas Cy5-loaded albumin nanoparticles showed diffuse fluorescence throughout the cell (Fig. 2b-c). The latter observation was attributed to the release of Cy5 dye bound non-covalently to nanoparticles following nanoparticle internalization. The punctual structures in the cytosol represented individual or aggregated nanoparticles (Fig. 2c and Movie 5), presumably into lyso-endosomal compartments. Conjugation of Cy5 to albumin nanoparticles also exhibited the same punctual structures in adherent neutrophils as Alexa Fluor 647-conjugated albumin nanoparticles (Fig. 2c-d); thus, the dye conjugation method prevents dye dispersal following nanoparticle internalization. Comparing the fluorescence intensities of internalized Cy5-loaded nanoparticles with Cy5-conjugated nanoparticles, uptake efficiency of two types of albumin nanoparticles was similar (Fig. 2d). Further, we observed that the general morphology of the adherent neutrophils internalizing either type of nanoparticle was the same and cells had a similar surface area of  $54 \pm 6$  (mean  $\pm$  SD)  $\mu\text{m}^2$ . Unlike nanoparticles made from denatured albumin, native albumin-conjugated polystyrene nanoparticles remained bound to the surface of neutrophils without internalizing (Fig. 2e and Movie 6). We also did not observe uptake of albumin itself following intravenous infusion of Cy5 conjugated to albumin (Fig. 2f). As quantified by multiple images, 95% of all adherent neutrophils similarly internalized either dye-loaded or dye-conjugated albumin nanoparticles. In contrast, neither albumin-conjugated polystyrene particles nor Cy5-conjugated albumin was internalized by the adherent neutrophils (Fig. 2g).

Fc $\gamma$ Rs bind IgG-opsonized particles and denatured proteins, and activate endocytosis<sup>14</sup>. Thus, we investigated whether nanoparticles made of denatured albumin could be

internalized through Fc $\gamma$ R signaling. Using neutrophils obtained from *Fc $\gamma$ RIII<sup>-/-</sup>* mice, we observed that the uptake of albumin nanoparticles was significantly reduced compared to wild-type (WT) mice (Fig. 3a). On measuring the fluorescence intensity of Cy5-loaded albumin nanoparticles per neutrophil, we obtained a distribution of nanoparticle uptake per neutrophil (Fig. 3b). Fc $\gamma$ RIII contributed to ~50% of total uptake of albumin nanoparticles (Fig. 3g), consistent with the role of Fc $\gamma$ R signaling as a mechanism of immune complex internalization by neutrophils<sup>20</sup>. The basis of residual uptake is unclear but may involve other Fc $\gamma$  receptors<sup>21</sup>. Macrophage antigen-1 (Mac-1 or  $\alpha$ M $\beta$ 2 integrin) and lymphocyte function-associated antigen-1 (LFA-1 or  $\alpha$ L $\beta$ 2 integrin) mediate neutrophil adhesion during vascular inflammation and denatured albumin binds to Mac-1 and may contribute to uptake of denatured proteins<sup>14</sup>; however, we observed that the deletion of Mac-1 and LFA-1 had no effect on uptake of albumin nanoparticles (Fig. 3c-g).

We next examined whether albumin nanoparticles loaded with the Syk inhibitor, piceatannol<sup>15</sup>, could reverse the TNF- $\alpha$ -mediated firm adhesion of neutrophils to venular endothelial cells, and thus mitigate inflammation. Syk signaling is crucial in the mechanism of 'outside-in' integrin signaling that mediates  $\beta$ 2 integrin-dependent neutrophil adhesion, spreading and migration<sup>15,22</sup>. Piceatannol selectively inhibits Syk activity but it is an ineffective due to water solubility<sup>23</sup>. We investigated whether piceatannol could be loaded into albumin nanoparticles for delivery into adherent neutrophils (Supplementary Fig. S5). In this study, most neutrophils adhered to the endothelium, although a few rolling neutrophils were also seen (Fig. 4a and Movie 7). Intravenous infusion of piceatannol-loaded albumin nanoparticles, 1 mg/kg body weight of piceatannol (50  $\mu$ M), significantly reduced the number of adherent neutrophil and concomitantly increased the number of rolling cells (Fig. 4b-c and Movie 8). In controls, albumin nanoparticles alone had no effect (Fig. 4d).

To investigate further the mechanisms of action of piceatannol-loaded albumin nanoparticles, the flow chamber assay was used in which mouse neutrophils interacted with a monolayer of TNF- $\alpha$ -activated mouse lung endothelial cells under shear conditions. In control experiments, Cy5-loaded albumin nanoparticles were internalized by Gr-1 positive neutrophils as in the mouse venular studies. The nanoparticle signal was slightly increased in neutrophils stimulated with N-formyl methionyl peptide, formyl-methionyl-leucyl phenylalanine (fMLF) (Supplementary Fig. S6). However, treatment of neutrophils with piceatannol-loaded albumin nanoparticles, 800  $\mu$ g/ml (200  $\mu$ M as piceatannol) under shear conditions markedly reduced  $\beta$ 2 integrin-mediated neutrophil spreading and migration across TNF- $\alpha$ -activated endothelial cells and inhibited neutrophil adhesion (Fig. 4e). Thus, piceatannol-loaded albumin nanoparticles function by inhibiting  $\beta$ 2 integrin-mediated 'outside-in' signaling through Syk signaling, consistent with the known function of Syk<sup>15</sup>. Syk phosphorylation in fMLF-stimulated neutrophils was also abrogated in neutrophils internalizing piceatannol-loaded albumin nanoparticles (Fig. 4f) indicating that the drug loaded into nanoparticles blocked Syk activity. We performed a 3-(4,5-Dimethylthiazol-2-yl)-2,5-diphenyl tetrazolium bromide (MTT) assay<sup>24</sup> to eliminate possible drug toxicity effect. Incubating neutrophils with piceatannol-loaded albumin nanoparticles, 800  $\mu$ g/ml (200  $\mu$ M as piceatannol), did not affect cell viability (Fig. 4g). Thus, piceatannol-loaded

albumin nanoparticles inhibited Syk phosphorylation, and thereby impaired  $\beta 2$  integrin-mediated 'outside-in' signaling required for neutrophil spreading and migration.

Excessive accumulation of neutrophils in lungs is a major factor in the pathogenesis of acute lung injury associated with sepsis<sup>25</sup>. We showed that  $\beta 2$  integrin-dependent neutrophil adhesion to lung endothelial cells<sup>26</sup> contributes to acute lung injury<sup>4</sup>. Thus, we determined whether piceatannol-loaded albumin nanoparticles could ameliorate lung neutrophil infiltration induced by the intraperitoneal injection of LPS (lipopolysaccharide, 10 mg/kg body weight). Treating mice with piceatannol-loaded albumin nanoparticles, 4.3 mg/kg body weight as piceatannol (200  $\mu$ M in blood), 2 hr after LPS challenge, markedly reduced lung tissue myeloperoxidase (MPO) activity, an indication of reduced neutrophil sequestration (Fig. 4h, Fig. 4i, and Supplementary Fig. S7). Infiltration of both neutrophils and monocytes determined by bronchoalveolar lavage was also reduced by treating mice with piceatannol-loaded albumin nanoparticles (4.3 mg/kg body weight as piceatannol) (Fig. 4j). Comparison of MPO activity in LPS-induced lung inflammation after administration of piceatannol-loaded albumin nanoparticles and piceatannol (free drug) alone also showed that piceatannol-loaded nanoparticles were far more efficacious than piceatannol (Fig. 4k). Since as shown albumin nanoparticles are preferentially internalized by neutrophils *in vivo*, these results demonstrate that impaired neutrophil infiltration in lungs by piceatannol-loaded albumin nanoparticles is essential for inhibiting monocyte infiltration. These results also showed the utility of albumin nanoparticle loading of piceatannol for the treatment of acute lung injury.

In summary, we demonstrated an albumin nanoparticle approach for the delivery of drugs into inflammatory neutrophils adherent to endothelial cells that is in part dependent on Fc $\gamma$ RIII signaling. Adhesion of neutrophils to activated endothelial cells was required for the internalization of albumin nanoparticles. Since Fc $\gamma$ Rs are highly expressed in adherent neutrophils during inflammation and vascular diseases<sup>27</sup>, nanoparticles made of denatured albumin can be used to target inflammatory neutrophils while sparing the essential host-defense function of circulating neutrophil. This strategy limits the undesirable effects of globally blocking the essential bactericidal function of neutrophils. Furthermore, we suggest the feasibility of using albumin nanoparticles to target activated neutrophils without conjugating ligands or antibodies to the nanoparticle surface<sup>3,10</sup>. The results provide a proof-of-concept of a novel nanoparticle-based therapeutic approach for targeting activated neutrophils to treat a range of inflammatory disorders.

## Methods

### Preparation of albumin nanoparticles loaded with fluorescent dyes or piceatannol

BSA (bovine serum albumin) nanoparticles were prepared by the desolvation technique (Supplementary Fig. S1)<sup>16</sup>. BSA was first dissolved at a concentration of 20 mg/ml in deionized water. BSA solution, 1 ml, was used to make nanoparticles by the continuous addition of 3.5 ml of ethanol under stirring (650 rpm) for 10 min at RT. In some experiments, BSA solution at 20 mg/ml (1 ml) was mixed and incubated with 40  $\mu$ l of Cy5 dye (5 mg/ml) in chloroform for 1 hr, followed by desolvation with ethanol. To make piceatannol-loaded albumin nanoparticles, 1 ml of 20 mg/ml of BSA solution was incubated

with 1 mg of piceatannol dissolved in DMSO for 1 hr. To form stable albumin nanoparticles with or without a dye or piceatannol, BSA molecules were cross-linked by adding 20  $\mu$ l of 0.2% glutaraldehyde in the suspension. The suspension was stirred overnight at RT. Nanoparticle suspension was centrifuged at 14,000 rpm for 20 min at 4°C. After drying albumin nanoparticles, we obtained 80-90% albumin to form the nanoparticles. The nanoparticle pellet was re-suspended in water or phosphate-buffered saline, pH 7.4 for the study.

To measure the efficiency of piceatannol incorporation in BSA nanoparticles, different concentrations of piceatannol were added in the initial albumin solution. After centrifugation of suspension of piceatannol-loaded BSA nanoparticles at 14,000 rpm at 4°C for 30 min, the supernatant (containing unbound piceatannol) was collected and centrifuged using Microcon (10-kD cut-off) to separate unbound piceatannol from free BSA molecules. Piceatannol molecules were quantified by measuring the absorbance at 328 nm as shown in Supplementary Fig. S5. The loading yield of piceatannol in albumin nanoparticles was calculated by the following equation: Loading yield (%) = (Drug used- unloaded drug)/Drug used. After drying and weighting piceatannol-loaded albumin nanoparticles, we obtained 10-14 wt% of piceatannol loaded in albumin nanoparticles.

To conjugate covalently Alexa Fluor-647 or Cy5 dye to albumin nanoparticles, we used the carboxyl-amine reaction between dye and albumin<sup>19</sup>. After albumin nanoparticles were made using the desolvation method as described above, we mixed Alex Fluor 647-NHS with albumin nanoparticles, and incubated the mixture for 2 hr at RT. We centrifuged albumin nanoparticles to remove free dye molecules to obtain Alexa Fluor 647-conjugated albumin nanoparticles.

### Real-time fluorescence intravital microscopy

In vivo intravital microscopy was performed as described<sup>13</sup>. TNF- $\alpha$  (0.5  $\mu$ g in 250  $\mu$ l saline) was intrascrotally injected into wild-type (WT) or knockout mice. At 3 hr after TNF- $\alpha$  injection, mice were anesthetized with intraperitoneal injection of the mixture of ketamine (80 mg/kg), xylazine (2 mg/kg), and acepromazine (2 mg/kg) and maintained at 37°C on a thermo-controlled rodent blanket and a tracheal tube was inserted. After excision of the scrotum, cremaster muscles were exteriorized on the intravital microscope table. The cremaster preparation was superfused with thermo-controlled (37°C) and aerated (95% N<sub>2</sub>, 5% CO<sub>2</sub>) bicarbonate-buffered saline during the experiment. Fluorescently-labeled albumin nanoparticles (100  $\mu$ g) in 100  $\mu$ l of saline were infused through a cannula placed in a jugular vein, followed by infusion of the Alexa Fluor 488-labeled anti-mouse Gr-1 antibody (0.05  $\mu$ g/g body weight). Rolling and adherent neutrophils were monitored in an area of 0.02 mm<sup>2</sup> in inflamed cremaster muscle venules. Images were recorded using an Olympus BX61W microscope with a 60  $\times$  /1.0 NA water immersion objective lens and a high speed camera (Hamamatsu C9300) connected to an intensifier (Video Scope International). To study the therapeutic effects of piceatannol-loaded albumin nanoparticles, the Alexa Fluor 488-labeled anti-mouse Gr-1 antibody was intravenously infused, followed by infusion of either piceatannol-loaded albumin nanoparticles or control albumin nanoparticles (150  $\mu$ g of albumin nanoparticles containing 50  $\mu$ M piceatannol). At 30 or 60 minutes after infusion of

nanoparticles, rolling and adherent neutrophils were monitored. In some experiments, an Alexa Fluor 488-labeled anti-mouse F4/80 antibody (2 µg/mouse) was infused to monitor monocytes. Neutrophils that remained stationary or did not exceed displacement of > 8 µm for at least 30 sec were considered adherent. To quantify neutrophil rolling and adherence, each vessel was monitored for > 3 min. Approximately 20 venules from 3 mice were monitored for each group of experiments. Data analysis was performed using Slidebook 5.5 (Intelligent Imaging Innovations). To quantify fluorescence signals, we integrated fluorescence intensities of albumin nanoparticles internalized into neutrophils using the software, and analyzed the distribution of nanoparticle uptake in neutrophils.

*In vitro* cytotoxicity, Syk phosphorylation, flow cytometric analysis, flow chamber assay, and acute lung inflammation model are presented in Supplementary Methods.

### Statistical Analysis

Data are expressed as mean ± SD or SEM. Data were analyzed using one-way ANOVA (multiple groups) or Student *t*-test (two groups) of Origin 8.5, with *p* values <0.05 were considered significant.

### Supplementary Material

Refer to Web version on PubMed Central for supplementary material.

### Acknowledgments

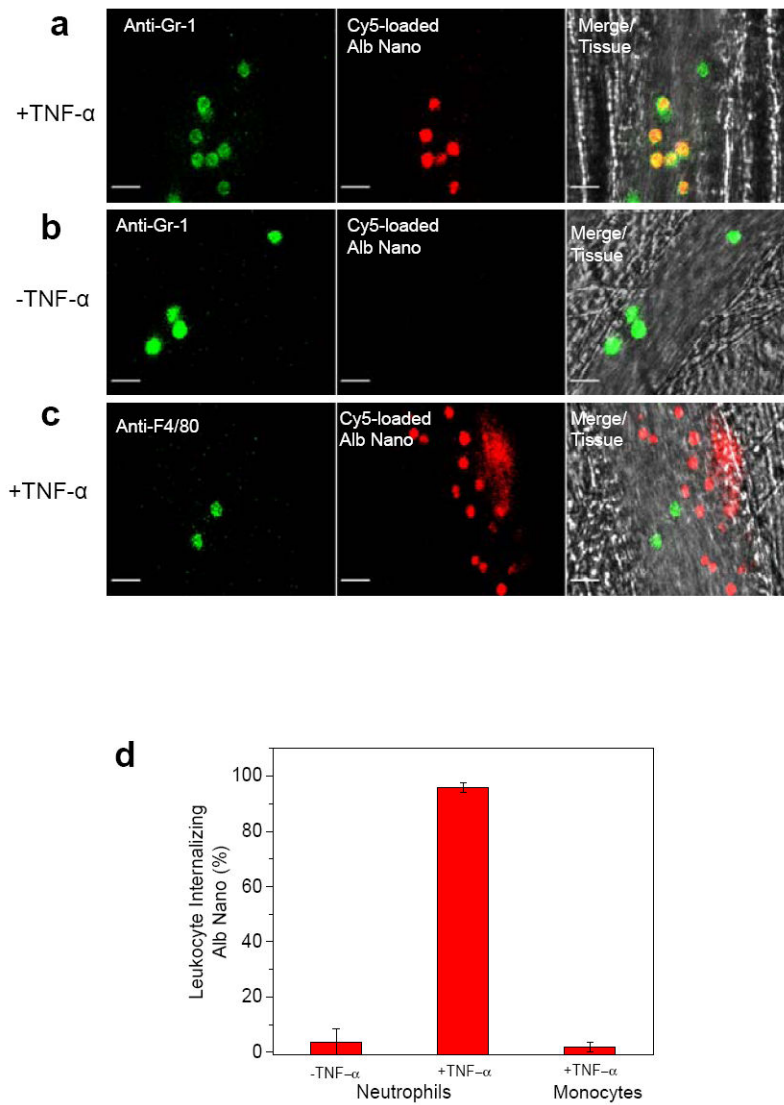
This work was supported by 11SDG7490013 from American Heart Association and NIH K25HL111157 to Z.W., R01 HL109439 to J.C., and P01 P01HL77806 to A.B.M.

### References

1. Hu G, Malik AB, Minshall RD. Toll-like receptor 4 mediates neutrophil sequestration and lung injury induced by endotoxin and hyperinflation. *Crit Care Med.* 2010; 38:194–201. [PubMed: 19789446]
2. Tabas I, Glass CK. Anti-inflammatory therapy in chronic disease: challenges and opportunities. *Science.* 2013; 339:166–172. [PubMed: 23307734]
3. Wang Z, Tirupathi C, Cho J, Minshall RD, Malik AB. Delivery of nanoparticle: complexed drugs across the vascular endothelial barrier via caveolae. *IUBMB Life.* 2011; 63:659–667. [PubMed: 21766412]
4. Xu J, et al. Nonmuscle myosin light-chain kinase mediates neutrophil transmigration in sepsis-induced lung inflammation by activating beta2 integrins. *Nat Immunol.* 2008; 9:880–886. [PubMed: 18587400]
5. Wong CH, Heit B, Kubes P. Molecular regulators of leucocyte chemotaxis during inflammation. *Cardiovasc Res.* 2010; 86:183–191. [PubMed: 20124403]
6. Phillipson M, Kubes P. The neutrophil in vascular inflammation. *Nat Med.* 2011; 17:1381–1390. [PubMed: 22064428]
7. Wagner DD, Frenette PS. The vessel wall and its interactions. *Blood.* 2008; 111:5271–5281. [PubMed: 18502843]
8. Lockwood CM, et al. Anti-adhesion molecule therapy as an interventional strategy for autoimmune inflammation. *Clin Immunol.* 1999; 93:93–106. [PubMed: 10527685]

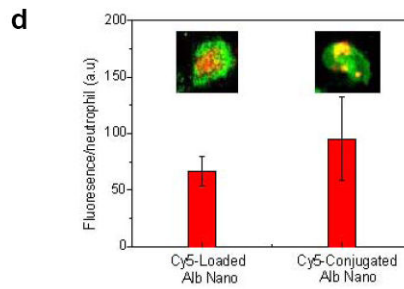
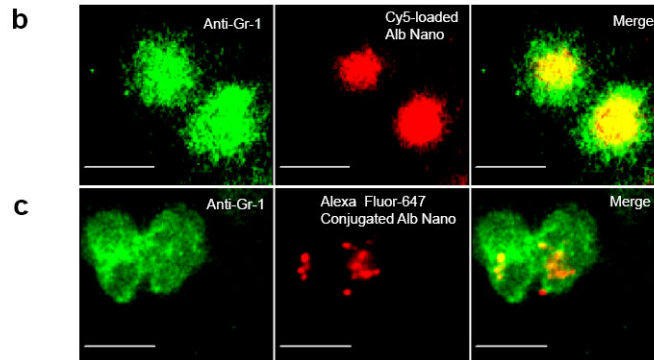
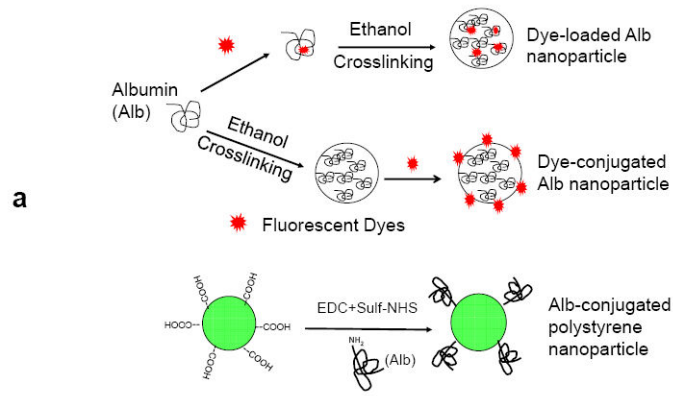
9. Sharar SR, Winn RK, Murry CE, Harlan JM, Rice CL. A CD18 monoclonal antibody increases the incidence and severity of subcutaneous abscess formation after high-dose *Staphylococcus aureus* injection in rabbits. *Surgery*. 1991; 110:213–219. [PubMed: 1677492]
10. Petros RA, DeSimone JM. Strategies in the design of nanoparticles for therapeutic applications. *Nat Rev Drug Discov*. 2010; 9:615–627. [PubMed: 20616808]
11. Farokhzad OC, Langer R. Impact of nanotechnology on drug delivery. *ACS Nano*. 2009; 3:16–20. [PubMed: 19206243]
12. Schroeder A, et al. Treating metastatic cancer with nanotechnology. *Nat Rev Cancer*. 2012; 12:39–50. [PubMed: 22193407]
13. Hahm E, et al. Extracellular protein disulfide isomerase regulates ligand-binding activity of alphaMbeta2 integrin and neutrophil recruitment during vascular inflammation. *Blood*. 2013; 121:3789–3800. [PubMed: 23460613]
14. Hidalgo A, et al. Heterotypic interactions enabled by polarized neutrophil microdomains mediate thromboinflammatory injury. *Nat Med*. 2009; 15:384–391. [PubMed: 19305412]
15. Evans R, Lellouch AC, Svensson L, McDowall A, Hogg N. The integrin LFA-1 signals through ZAP-70 to regulate expression of high-affinity LFA-1 on T lymphocytes. *Blood*. 2011; 117:3331–3342. [PubMed: 21200022]
16. Weber C, Kreuter J, Langer K. Desolvation process and surface characteristics of HSA-nanoparticles. *Int J Pharm*. 2000; 196:197–200. [PubMed: 10699717]
17. Sumagin R, Prizant H, Lomakina E, Waugh RE, Sarelius IH. LFA-1 and Mac-1 define characteristically different intraluminal crawling and emigration patterns for monocytes and neutrophils in situ. *J Immunol*. 2010; 185:7057–7066. [PubMed: 21037096]
18. Bull HB, Breese K. Interaction of Alcohols with Proteins. *Biopolymers*. 1978; 17:2121–2131.
19. Wang Z, Tirupathi C, Minshall RD, Malik AB. Size and dynamics of caveolae studied using nanoparticles in living endothelial cells. *ACS Nano*. 2009; 3:4110–4116. [PubMed: 19919048]
20. Chen K, et al. Endocytosis of soluble immune complexes leads to their clearance by Fc gammaRIIIB but induces neutrophil extracellular traps via Fc gammaRIIA in vivo. *Blood*. 2012; 120:4421–4431. [PubMed: 22955924]
21. Indik ZK, Park JG, Hunter S, Schreiber AD. The molecular dissection of Fc gamma receptor mediated phagocytosis. *Blood*. 1995; 86:4389–4399. [PubMed: 8541526]
22. Zarbock A, Lowell CA, Ley K. Spleen tyrosine kinase Syk is necessary for E-selectin-induced alpha(L)beta(2) integrin-mediated rolling on intercellular adhesion molecule-1. *Immunity*. 2007; 26:773–783. [PubMed: 17543554]
23. Geahlen RL, McLaughlin JL. Piceatannol (3,4,3',5'-tetrahydroxy-trans-stilbene) is a naturally occurring protein-tyrosine kinase inhibitor. *Biochem Biophys Res Commun*. 1989; 165:241–245. [PubMed: 2590224]
24. Wisel S, et al. Pharmacological preconditioning of mesenchymal stem cells with trimetazidine (1-[2,3,4-trimethoxybenzyl]piperazine) protects hypoxic cells against oxidative stress and enhances recovery of myocardial function in infarcted heart through Bcl-2 expression. *J Pharmacol Exp Ther*. 2009; 329:543–550. [PubMed: 19218529]
25. Matthay MA, Zemans RL. The acute respiratory distress syndrome: pathogenesis and treatment. *Annu Rev Pathol*. 2011; 6:147–163. [PubMed: 20936936]
26. Lo SK, Everitt J, Gu J, Malik AB. Tumor necrosis factor mediates experimental pulmonary edema by ICAM-1 and CD18-dependent mechanisms. *J Clin Invest*. 1992; 89:981–988. [PubMed: 1347298]
27. Nakatani K, et al. Regulation of the expression of Fc gamma receptor on circulating neutrophils and monocytes in Kawasaki disease. *Clin Exp Immunol*. 1999; 117:418–422. [PubMed: 10444279]





**Figure 1. Uptake of albumin nanoparticles by adherent neutrophils in venules**

Intravital microscopy of mouse cremaster muscle venules demonstrates that Cy5-loaded albumin nanoparticles (red) are internalized by activated neutrophils following TNF- $\alpha$  (0.5  $\mu$ g/mouse) (a) or during surgical stress-induced (b) vascular inflammation in mice. Neutrophils (green) were visualized by intravenous infusion of Alexa Fluor 488 anti-mouse Gr-1 antibody. In the TNF- $\alpha$  challenge group, the nanoparticles were intravenously infused 3 hr post-intrascrotal injection of TNF- $\alpha$  (0.5  $\mu$ g/mouse). c, Monocytes (green) were visualized by infusion of Alexa Fluor 488 anti-mouse F4/80 antibody also 3hr following TNF- $\alpha$ -induced vascular inflammation. Scale bars, 20  $\mu$ m. d, Percentage of neutrophils and monocytes internalizing albumin nanoparticles. In all experiments, 100  $\mu$ g fluorescent dye-labeled albumin nanoparticles was infused intravenously per mouse. All data represent mean  $\pm$  SEM (n = 13-20 vessels in 3 mice per group).



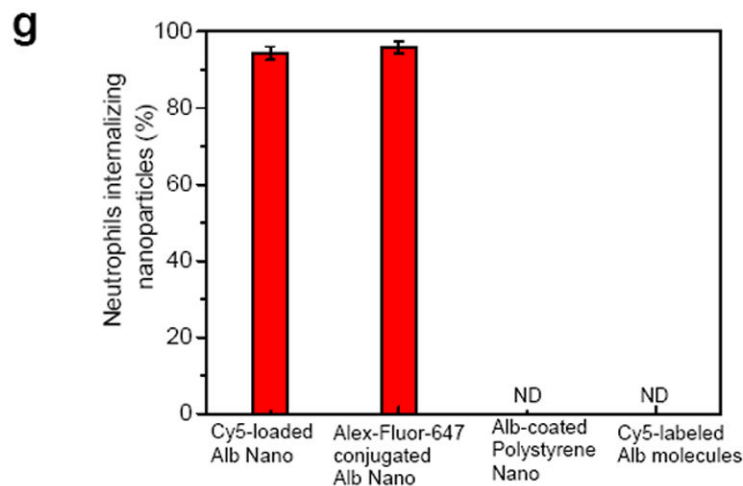
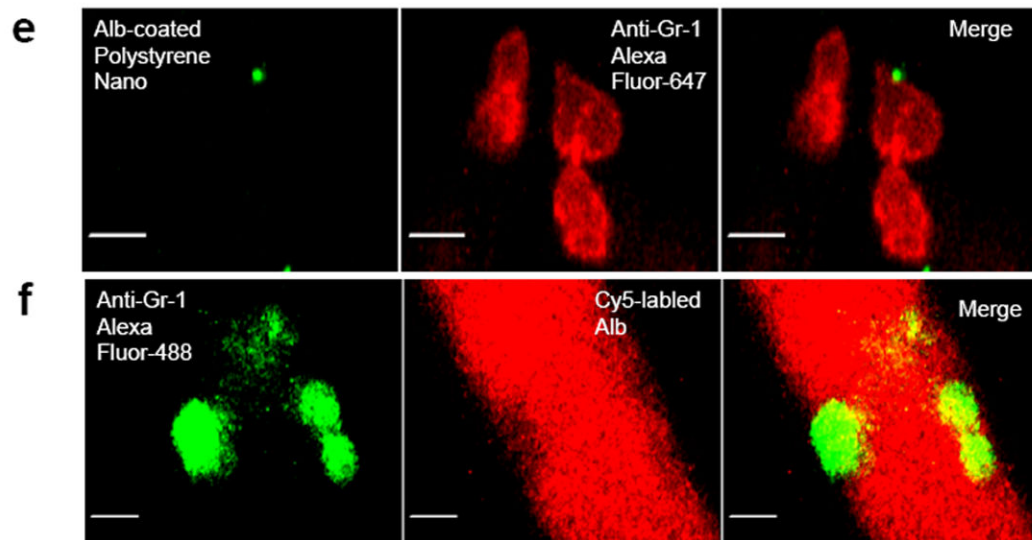


**Figure 2. Characteristics of internalization properties of different types of albumin nanoparticles**

**a.** Formulation of three types of fluorescently-labeled albumin nanoparticles studied.

Albumin nanoparticles made from denatured albumin were either loaded with Cy5 (Dye-loaded Alb nanoparticle) or the particle surface was chemically conjugated with Alex Fluor 647 or Cy5 (Dye-conjugated Alb nanoparticle) as described in Methods. The third type is polystyrene nanoparticles (also with diameter of 100 nm) made by conjugating with native albumin (Alb-conjugated polystyrene nanoparticle). Intravital microscopy was performed in mice as described in Fig. 1. Cy5-loaded (**b**) and Alex Fluor 647-conjugated (**c**) albumin nanoparticles (red) were internalized by Gr-1-positive neutrophils (green). Scale bars, 10  $\mu$ m. **d.** Quantitative analysis of uptake of Cy5-loaded and Cy5-conjugated albumin nanoparticles was carried out by measuring fluorescence intensity per neutrophil. Inset images show Cy5-loaded and Cy5-conjugated albumin nanoparticles (red) internalized by

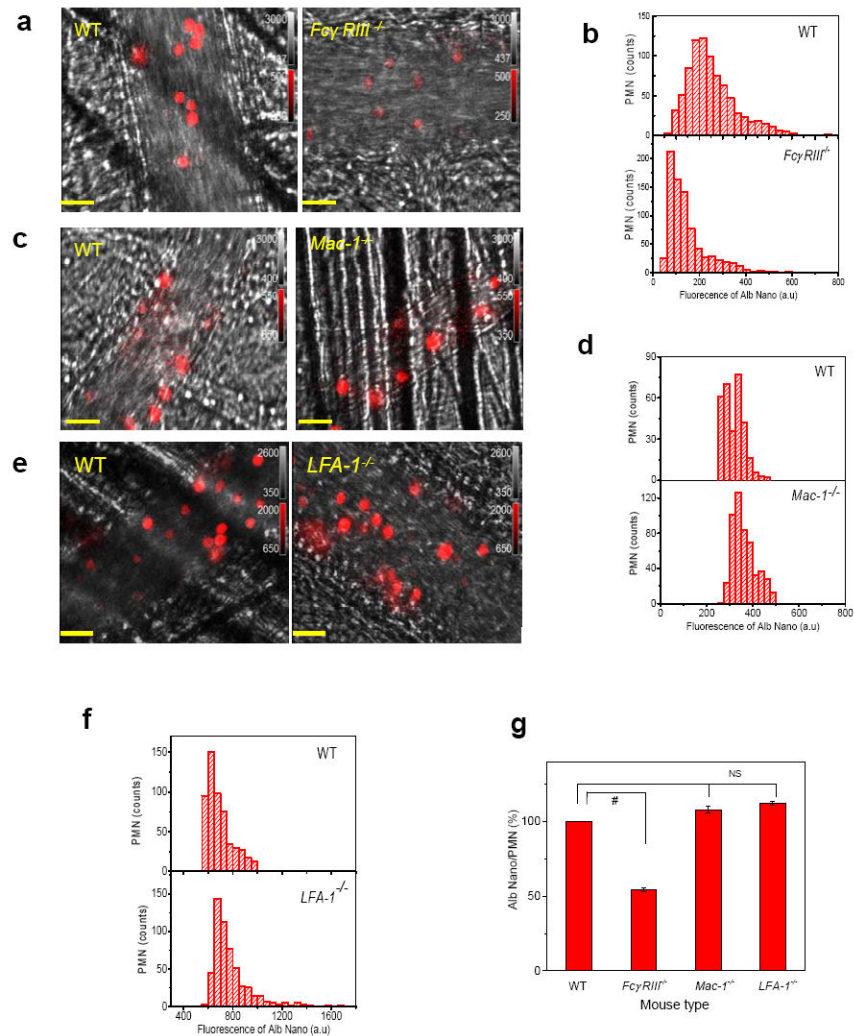
neutrophils (green). **e**, Native albumin-conjugated polystyrene nanoparticles (green) were bound to the neutrophil surface (red). **f**, Cy5-conjugated native albumin (red) was not internalized by Gr-1-positive neutrophils (green). Scale bars, 10  $\mu\text{m}$ . **g**, Quantitative analysis of percentage of Gr-1-positive neutrophils internalizing the 3 types of nanoparticles and Cy5-labeled albumin. Results are shown as mean  $\pm$  SEM (n = 13-20 vessels in 3 mice per group). ND = not detected.

Author Manuscript

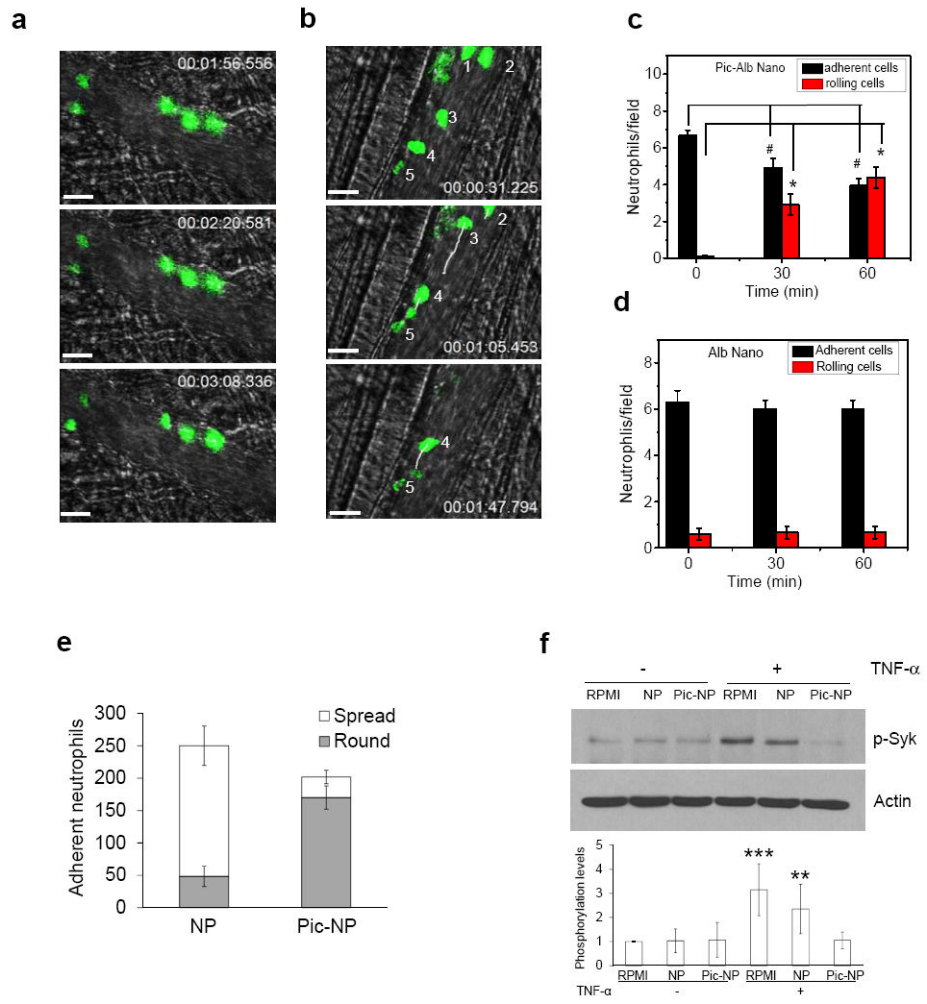
Author Manuscript

Author Manuscript

Author Manuscript



**Figure 3. Contribution of FcγRIII mechanism in mediating albumin nanoparticle internalization**  
**a-f**, Intravital microscopy of cremaster muscle inflamed venules was performed in wild-type (WT) and *FcγRIII*<sup>-/-</sup> (**a**), *Mac-1*<sup>-/-</sup> (**c**), and *LFA-1*<sup>-/-</sup> mice (**e**). Scale bars, 20 μm. Cy5-loaded albumin nanoparticles (red) were intravenously infused 3 hr after the intrascrotal injection of TNF-α (0.5 μg/mouse). Histograms of Cy5-loaded albumin nanoparticles internalized by neutrophils in WT and *FcγRIII*<sup>-/-</sup> (**b**), *Mac-1*<sup>-/-</sup> (**d**), and *LFA-1*<sup>-/-</sup> mice (**f**) were obtained from more than 500 neutrophils in 3 mice per group. Integrated fluorescence intensities of nanoparticles in individual polymorphonuclear neutrophils (PMNs). **g**, Percentage albumin nanoparticle uptake in WT versus knockout mice in each group based on data from (**b**, **d**, and **f**). Results are shown as mean ± SEM. # P<0.0001 vs. WT mice after ANOVA and Dunnett's test. NS, not significant.



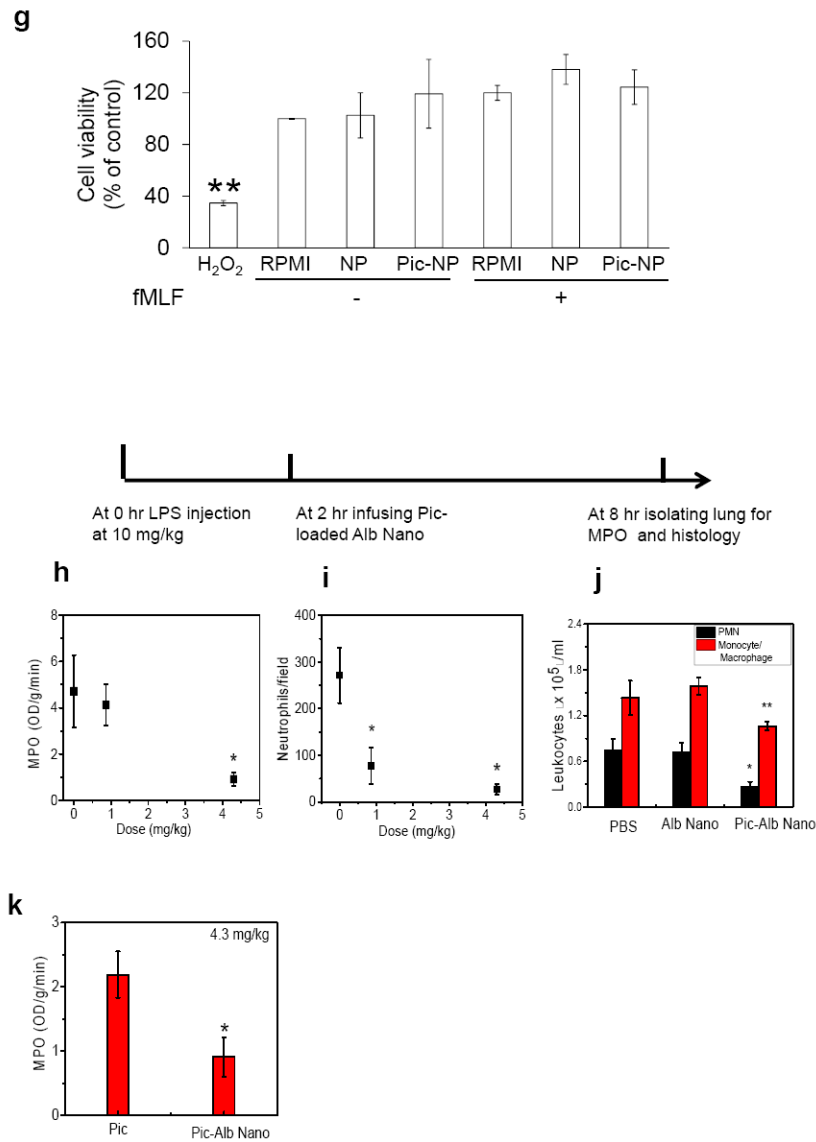


**Figure 4. Therapeutic activity of albumin nanoparticles in vascular inflammation and lung injury models**

**a-d**, Intravital microscopy showing rolling and adhesion of neutrophils (green) monitored by intravenous infusion of Alexa Fluor 488-conjugated antibodies in mice before **(a)** and at 1 hr post-intravenous infusion of piceatannol-loaded albumin nanoparticles (50  $\mu$ M piceatannol) **(b)** in the same mouse. hh:mm:ss in **(a)** and **(b)** represent time series of images. Numbers in **(b)** represent neutrophils. White lines show trajectories of neutrophils detaching from endothelial cells. Scale bars, 20  $\mu$ m. **c**, Quantification of neutrophil adhesion and rolling in TNF- $\alpha$ -activated cremaster muscle vessels at baseline and at 30 and 60 min after intravenous infusion of piceatannol-loaded albumin nanoparticles. Data represent mean  $\pm$  SEM (n = 21 venules in 3 mice). # and \* represent P < 0.001 and < 0.001 vs. pre-infusion of piceatannol-loaded albumin nanoparticles after ANOVA and Dunnett's test. **d**, Albumin nanoparticles without piceatannol loading were tested as controls and quantified as described in **(c)**. Data represent mean  $\pm$  SEM (n = 18 venules in 3 mice). **e**, Mouse

neutrophils were pre-treated with 800  $\mu\text{g/ml}$  albumin nanoparticles (NP) or piceatannol-loaded albumin nanoparticles (Pic-NP, 200  $\mu\text{M}$  as piceatannol), and stimulated with N-formyl-methionyl-leucyl-phenylalanine (fMLF). Flow chamber assay at fixed shear representing venous shear (1 dyne/cm<sup>2</sup>) was performed as described in Supplementary Methods. The number of adherent neutrophils (either spread or round) was quantified during the 10-min recording period. Data represent mean  $\pm$  SD (n = 3). **f**, Mouse neutrophils were plated on fibrinogen-coated surfaces and incubated with RPMI culture media, 800  $\mu\text{g/ml}$  albumin nanoparticles (NP) or piceatannol-loaded albumin nanoparticles (Pic-NP, 200  $\mu\text{M}$ ) in the presence of 50 ng/ml TNF- $\alpha$  for 30 min. Lysates were immunoblotted with anti-phospho Syk-Tyr525/526 antibody. Data represent mean  $\pm$  SD (n = 3). \*\*  $P < 0.01$  and \*\*\*  $P < 0.001$  vs. unstimulated cells after ANOVA and Dunnett's test. **g**, Unstimulated or fMLF-stimulated mouse neutrophils were treated with 800  $\mu\text{g/ml}$  albumin nanoparticles (NP) or piceatannol-loaded albumin nanoparticles (Pic-NP, 200  $\mu\text{M}$  as piceatannol) for 1 hr. MTT assay was performed as described in Methods. Cell viability is presented as mean  $\pm$  SD (n = 3). \*\*  $P < 0.01$  vs. unstimulated cells after ANOVA and Dunnett's test. Cell viability was not different among any experimental group. **h-k**, Effects of piceatannol-loaded albumin nanoparticles on LPS-induced lung inflammation (See Methods for details). The line above the figures describes the protocol. Lung myeloperoxidase (MPO) activity (**h**) and number of neutrophils sequestered in lungs (**i**) before and after intravenous infusion of piceatannol-loaded albumin nanoparticles. Data represent mean  $\pm$  SD (n = 3). \*  $P < 0.001$  vs control after ANOVA. **j**, Leukocyte number in bronchoalveolar lavage (BAL) after intravenous infusion of albumin nanoparticles (Alb-Nano) and piceatannol-loaded albumin nanoparticles (Pic-Alb Nano) with piceatannol amount at 4.3 mg/kg body weight. \*  $P < 0.01$  and \*\*  $P < 0.05$ . **k**, Neutrophil infiltration in LPS-induced acute lung inflammation assessed by MPO activity after intravenous infusion of piceatannol (Pic)-loaded albumin nanoparticles compared to free piceatannol, 4.3 mg/kg body weight. \*  $P < 0.05$  vs. free piceatannol after Student *t*-test.